Chapter 3
Fluorescence Microscopy

W. Gray (Jay) Jerome and Robert L. Price

3.1 Introduction

To harness the power of fluorescence for biological microscopic imaging, a number of additional components must be introduced to the standard light microscope. The most important modifications are (1) a strong illumination system that provides suitable wavelengths for exciting a specific fluorochrome, (2) some mechanism to limit the illumination beam to specific wavelengths so that only the fluorochrome of choice is excited, and (3) a means to image only the light emitted from the fluorochrome so that the excitation light (and other stray wavelengths) are not imaged. Inclusion of light from anything other than the fluorochrome would degrade the image fidelity and signal to noise ratio (SNR). In this chapter we will discuss a basic set up that meets the criteria for good fluorescent imaging. Subsequent chapters will expand on this theme and discuss additional modifications required specifically for laser scanning and spinning disk confocal fluorescence.

W. G. Jerome (✉)
Department of Pathology, Microbiology and Immunology, Vanderbilt University School of Medicine, Nashville, TN, USA
e-mail: Jay.Jerome@vanderbilt.edu

R. L. Price
Department of Cell Biology and Anatomy, University of South Carolina School of Medicine, Columbia, SC, USA
e-mail: Bob.Price@uscmed.sc.edu

W. G. Jerome, R. L. Price (eds.), *Basic Confocal Microscopy*,
https://doi.org/10.1007/978-3-319-97454-5_3

3.2 The Optical Path in a Fluorescence Microscope

In standard transmitted light microscopy, a beam of light is focused onto the specimen by a condenser located below the specimen (transillumination light path in Fig. 3.1). The light is altered as it traverses the specimen and this altered light is collected by the objective lens and transmitted ultimately to the imaging device (eye, camera, etc.). While this design can be used for fluorescence, there are significant problems involved in separating the excitation light from the light emitted by the fluorophore. Obviously, it is critical to image only the emitted light, since all other wavelengths are false signals that degrade image quality and might be incorrectly interpreted.

The separation of emitted light from other wavelengths is much easier when the emitted light is traveling in the opposite direction to the excitation light. For this

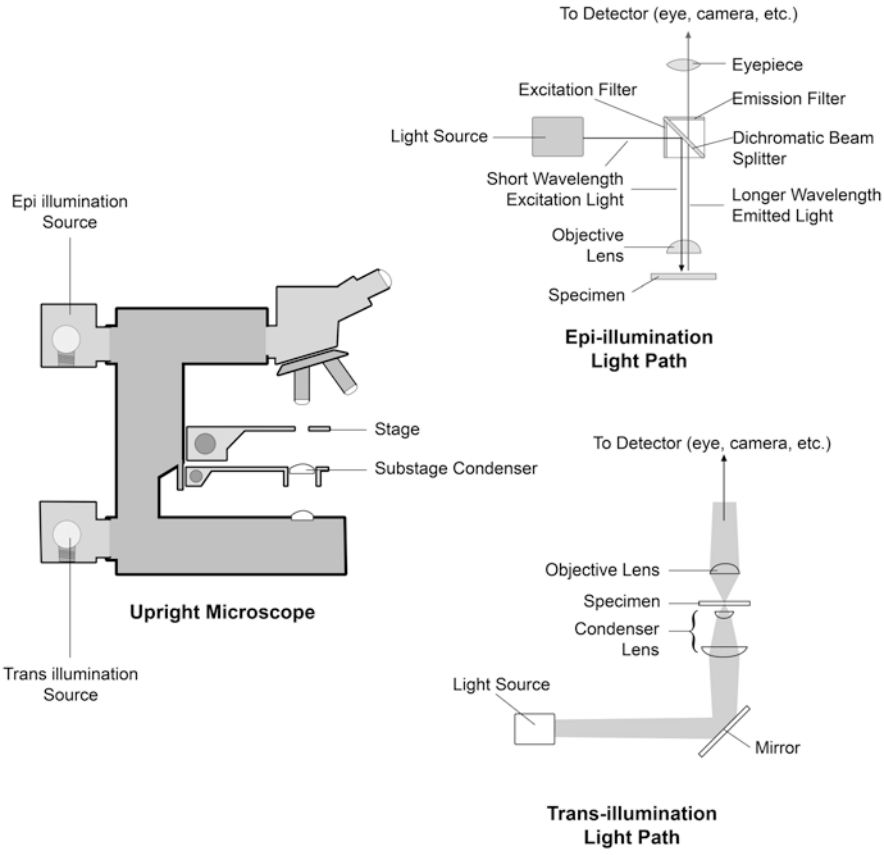

Fig. 3.1 Optical path in epi-illumination and transillumination microscope designs. Depicted here is the setup for an upright microscope. However, the trans- or epi-illumination design can be implemented just as easily with an inverted microscope

reason, most fluorescence is done using a type of illumination called epi-illumination (Fig. 3.1). In this design, the excitation illumination is focused onto the specimen by the objective lens rather than a condenser lens (i.e., the objective lens acts as a high-quality condenser lens). The objective lens is also used to collect and focus the light emitted by the fluorophore, just as it would be in a transilluminated light setup. By illuminating the specimen with incident light, the only excitation light in the imaging path is that which is reflected from the specimen or reflected from glass surfaces. When effectively minimized, the reflected light has a very minor intensity compared to the light emitted from the excited fluorochrome. Limiting reflection is a key component of successful epifluorescence microscopy. The incident light is further reduced by appropriate filters or other means that block its transmission to the imaging device (see Sect. 3.5). This epifluorescence strategy is useful for both wide-field and confocal fluorescence microscopy.

3.3 Light Sources

As indicated in Fig. 3.1, the light path for epi-illumination begins with the light source. A suitable light source must be able to provide a high photon flux at a wavelength that will excite the fluorochrome of interest. High levels of excitation are necessary because the fluorescence emission is usually low due to fluorochrome and specimen characteristics such as low quantum yield, limited labeling, and loss of light within the optical path of the microscope. These limitations are discussed later in this chapter and in the chapters on specimen preparation, immunolabeling, and system components. The bottom line is that one usually needs to maximally excite the fluorochrome in order to get a signal that is distinguishable from the general background noise level.

A second requirement of a fluorescence lamp is that the intensity of the illumination should be uniform at the back aperture of the objective lens. If it is not, uneven sample excitation and uneven brightness in the final image may result. This can also be a problem if the illuminating source is not properly aligned. Checking the source alignment on a regular basis should be a routine procedure.

Traditionally, two illumination sources that meet the above criteria of uniformity, intensity, and specificity have been employed: mercury arc lamps and xenon arc lamps. Both of these produce photons as the result of a voltaic arc running through an ionized gas. The mercury bulb produces photons with wavelengths that cover the full visible spectrum and the UV range, as well. For this reason, they are well suited for exciting fluorochromes with absorbance maxima below 380 nm as well as those with absorbance in the visible range. However, the intensity at different wavelengths is not uniform. Mercury arc lamps show peak intensities at 313, 334, 365, 406, 435, 546, and 578 nanometers (Fig. 3.2a). The intensities at other wavelengths are much lower. For this reason, when using a mercury lamp, it is best to carefully select fluorochromes that have good absorbance at, or close to, the peak wavelengths.

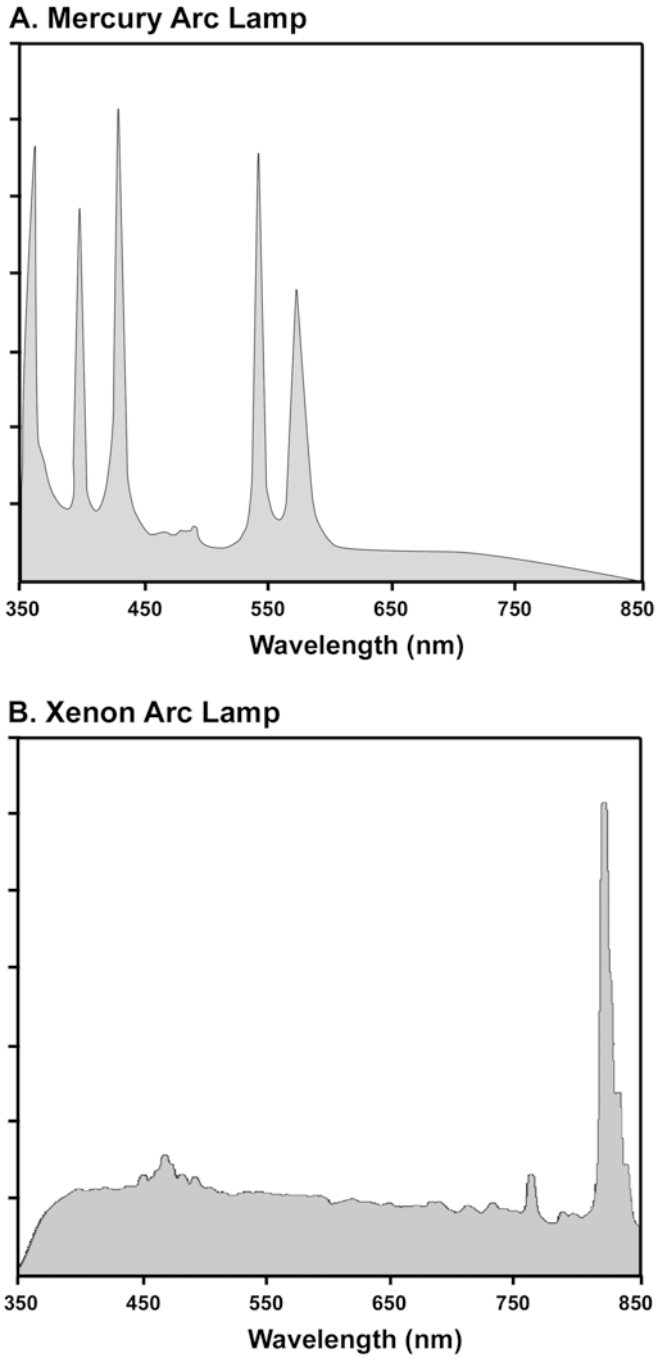

Fig. 3.2 Spectrum of light emitted from mercury arc (**a**) and xenon arc (**b**) lamps

Like mercury lamps, xenon lamps are arc lamps using an ionized gas to generate light. Xenon lamps have a more uniform distribution of intensities across the visible range, but their intensities fall off rapidly at wavelengths below 400 nm and so are less suitable for exciting fluorochromes with UV absorption (Fig. 3.2b). The intensities at peak wavelengths are also not as high as those from the most intense wavelengths of mercury lamps. Another drawback of xenon lamps is that they give off significant radiation in the infrared range which can produce excessive heat. This heat must be efficiently dissipated because excessive heat can damage specimens and can affect the characteristics of environmentally sensitive fluorochromes.

With both xenon and mercury lamps, one must keep track of the number of hours the bulbs have been used. Beyond the useful life of the bulb, the spectral emissions can change dramatically, altering the microscopy results. The increase in use of fluorescence microscopy, however, has spurred innovative approaches to improving arc lamp design. One such advancement has been the introduction of mercury arc lamps, such as the X-Cite ® series of lamps from EXFO (EXFO Photonic Solutions Inc. Ontario, Canada). These lamps include a cleaning cycle technology that removes burned material that tends to build up on the walls of arc lamps. This can greatly extend the useful life of the lamp by as much as tenfold.

Although arc lamps are very useful for fluorescence microscopy, they have their drawbacks. Chief among these are the relatively short life span, instability, and the need to filter out unwanted wavelengths. In addition, the heat from xenon lamps can be problematic for live cell imaging. In recent years, newer light sources have been introduced that overcome some of the issues with arc lamps. A particularly exciting change has been the development of high-performance light-emitting diodes (LEDs). The newest breeds of LEDs have several advantages over mercury or xenon arc lamps for fluorescence microscopy. Like arc lamps, LEDs have a high and stable output. However, they have very low energy consumption and generate less heat. They are also relatively inexpensive and have a very long useable life span. LEDs can produce light within narrow wavelengths, so filtering non-specific wavelengths is simplified. An array of LEDs can be employed to cover the spectrum from near UV through red; consequently the choice of fluorochromes is not limited. The drawback is that their light output is less intense than the output from arc lamps, but this parameter is improving rapidly, and newer LED systems now provide suitable photon flux for most fluorescent microscopy needs. A number of LED-based sources are now available for fluorescent confocal microscopy.

The use of arc burners and LED arrays in confocal microscopy are generally limited to spinning disk confocal microscopes. For single point scanning confocal microscopes, a laser is usually the light source of choice because of its high photon flux and physical properties. Laser is an acronym for *Light Amplification by Stimulated Emission of Radiation*. Chapter 2 discussed spontaneous emission of light. Laser light represents stimulated emission. This is a situation where an atom or molecule retains its excess energy until stimulated to emit the energy as light. Lasers both produce and amplify this stimulated form of light. Like spontaneous fluorescence, the emission is restricted to specific wavelengths that are dependent upon the material used for creating the light. Thus, most lasers produce an intense,

monochromatic beam that is coherent and highly collimated. The coherence of the beam introduces problems when used in standard wide-field microscopy because scattering and interfering diffraction patterns are produced at all of the surfaces in the optical path, including any dirt in the system. This is much less of a problem, however, when a tightly focused beam is rastered point-by-point across the specimen and the image information collected sequentially from each illuminated point. This is exactly the procedure utilized in single point scanning confocal microscopy.

At its simplest, a laser consists of a gain medium contained in a reflective optical cavity with an energy supply (Fig. 3.3). Light is generated within the cavity, and, by placing mirrors within the cavity, the light is reflected back and forth within the gain medium. This leads to an amplification of the energy. The energy for amplification (pumping) is usually supplied as an electrical current or light of a different wavelength.

The gain medium is a material capable of stimulated emission. It can be a gas, liquid, plasma, or solid. The gain medium absorbs the pumped energy resulting in electrons in the medium becoming excited. In spontaneous emission this energy would be rapidly lost, and the electrons would return to the ground state. In stimulated emission, the electrons maintain their higher energy state. When the number of excited state electrons exceeds those in a lower state, this is called population inversion. It is a requisite for laser emission. In this state, when a photon is absorbed, the energy released as the atom returns to the ground state will exceed the energy of the photons absorbed. Thus, the light is amplified. Because the injected light passes back and forth through the medium multiple times, the emission becomes greatly amplified.

Although there are a variety of materials that can be used as the gain medium in lasers, for general biological laser scanning confocal microscopy, gas lasers have

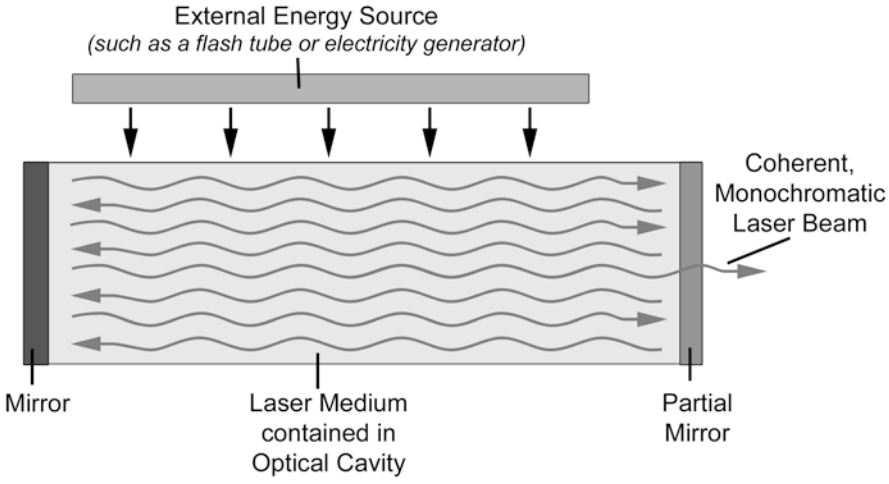

Fig. 3.3 Diagram of general laser principle

historically predominated. The most popular, because of available wavelengths, cost, and ease of operation, have been argon-ion and helium-neon lasers. Recently, however, the technology involved in other forms of lasers has advanced sufficiently to make them useful for laser scanning microscopy. In particular, titanium-doped sapphire (Ti:sapphire) solid state lasers have gained prominence for multiphoton excitation. For these lasers, sapphire is doped with titanium to provide the appropriate energy states for stimulated emission. Ti:sapphire lasers are tunable to a variety of wavelengths in the IR range and can be engineered to produce ultrashort pulses. These properties make them ideal for multiphoton excitation (see Chap. 2, Sect. 2.4).

Another form of laser is the diode laser. Diode lasers are semiconductor devices where a crystal substrate is doped with two very thin layers of material that will form positive (P) and negative (N) diode junctions (diodes). The difference in chemical potential between the n- and p-type semiconductors produces a depletion region at the interface. An electrical bias causes charge carriers (holes and electrons) to be injected into the depletion region from the p-doped (holes) and n-doped (electrons) sides. The recombination of electrons and holes in the depletion region produces photons which are stimulated by incident photons. The stimulation leads to amplification. The first diode lasers that were developed emitted mostly in the IR region. However, advances have increased the power output of diode lasers, and diodes that emit in the blue and red regions have been developed, making them useful for fluorescence microscopy. Diode lasers are now becoming common as the illumination source for newer confocal microscopes.

One of the strengths of lasers is the monochromatic nature of the emitted photons. For microscopy, the fact that the excitation light exists essentially as a single wavelength simplifies filtering of non-specific light. However, just like with LEDs, separate lasers are required for each excitation wavelength of interest. At best, a single laser may provide several suitable wavelengths (Fig. 3.4). Unlike LEDs, though, practical considerations, such as cost, usually limit the number of lasers provided with laser scanning confocal microscope systems. This means that a particular instrument usually is not equipped to cover the full visible spectrum and so

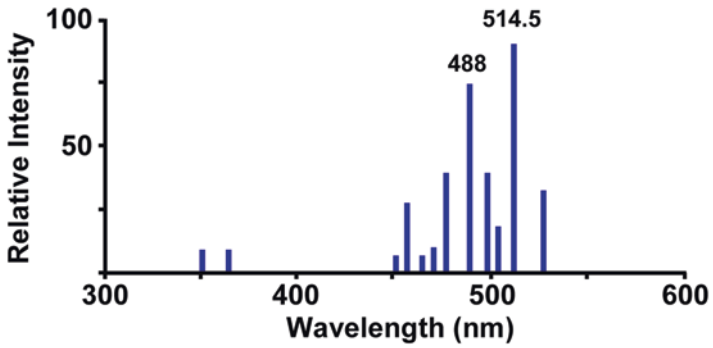

Fig. 3.4 Spectrum of light emitted from argon gas laser

one is limited in the choice of fluorochromes that can be employed. Luckily, fluorochrome manufacturers have realized an opportunity, and a great deal of work has been done in the last two decades to develop fluorochromes with properties that match the standard laser lines available with most laser scanning confocal microscopes. Thus the presence of limited wavelengths is no longer as restrictive to biological experiments as it was previously. Very recently, white light lasers have been introduced. These use a low energy-pulsed infrared fiber laser that is then amplified by a diode laser to produce wavelengths in the 450 to 670 range. An acoustic optical device is then employed to select specific narrow wavelengths for imaging. At present, these are very expensive but as the technology is developed and cost reduced their utility in confocal microscopy will increase.

3.4 Objective Lens Characteristics and Terminology

All components in the optical path are important in the collection of a high-quality confocal image. However, the objective lens may be the most critical element since the initial image is formed, the resolution determined, and most of the magnification of the final image is obtained via the objective. Even with an optimum specimen and the operating parameters of the confocal system set up properly, if the objective lens is of poor quality, or an improper lens used, the image will be inferior. While everyday users may not have control over the choice of available objectives on a core or established instrument, it is important to understand the optical characteristics of each available objective and how these characteristics may affect the collection and interpretation of the data. Only with this knowledge will you be able to select from your available choices a lens that is most suitable for your experimental needs. For example, if a limited number of objective lenses are available, it may be necessary to use a standard 40X oil immersion objective to collect data from both a cell culture sample and a 100 μm thick section of tissue labeled with multiple fluorochromes. However, this objective is a poor choice for imaging thick specimens if optional 40X water immersion optics are available.

So, how does one choose the optimal lens? In this section we give a number of examples demonstrating how the selection of an optimum objective lens can improve the acquisition, reconstruction, and interpretation of confocal data sets. However, before giving the examples, we will first provide several definitions and information about objectives that are essential in understanding why it is essential to have the correct optics on a confocal microscope for the acquisition of a given data set. Much of the discussion relates to a fundamental problem that we face when imaging; the optical components of our systems and the specimens we are trying to image have fundamentally different physical and chemical properties. This can result in refractive index mismatch as various wavelengths of light are affected differently as they pass through each component (Table 3.1).

With regard to confocal microscopy, refractive index refers to a measurement of how the wavelength of photons is affected as they pass through a substrate. This is

Table 3.1 Refractive index depends on concentration and molecular weight of proteins and nucleic acids (Voros 2004; Samoc et al. 2007). Mismatch of refractive indices of various components in the optical path results in significant loss of signal in confocal imaging

Substrate	Refractive index
Air	1.0
Water	1.32–1.34
Immersion oil	1.515
Glycerol (75%)	1.44
Polyvinyl alcohol	1.52–1.55
Protein[1]	1.36–1.5
Nucleic Acids[2]	1.5–1.6

Fig. 3.5 Effect of refractive index differences on the visualization of a straight pencil

important for two reasons. First, light rays change direction when they cross the interface from the objective to air or the immersion fluid used for immersion and dipping lenses. Second, light reflects partially from surfaces that have a refractive index different from that of their surroundings. Figure 3.5 shows a simple example of how refractive index mismatch can distort an image. Although the pencil is straight, its perceived image is dramatically distorted by the refractive index differences between air, glass, and water. Thus, it is critical to understand, minimize, and correct for refractive index differences.

The refractive index of each component in the optical path, including the optics of the objective lens, the filters used to separate the various wavelengths of photons, the immersion fluid or air the lens is designed to image through, the coverglass, the mounting medium of the specimen, and the specimen itself is specific and based on the molecular composition of the material. As photons, both excitatory and emitted, pass through each component, their path is affected. If the refractive indices of each component of the microscope and sample are not matched, refractive index mismatch occurs resulting in image aberrations and loss of specimen signal reaching

the detector (Dunn and Wang 2000; Diaspro et al. 2002). Some common refractive indices for various materials are given in Table 3.1. Optimizing microscope performance includes accounting for and minimizing the effects of refractive index differences in your image.

3.4.1 Objective Lens Inscriptions

Inscribed on all objectives is information concerning the objective specifications and information about the type of imaging for which the objective is optimized. Figure 3.6 shows several Zeiss and Nikon objectives. Inscribed on each is information concerning the type of lens; the magnification; the focal length; the numerical aperture (NA); if it is an immersion lens (Fig. 3.6b and c); whether it is corrected for use with water, oil, or glycerol; and the coverglass thickness for which the objective is corrected. Definitions and considerations important in lens selection for confocal imaging are presented below. Several images are also shown in the following sections which illustrate the importance of matching the correct objective with the goals of the experiment.

Plan objectives are flat-field objectives corrected to eliminate effects caused by curvature of the lens. Without correction, light from peripheral regions of the image will not be focused to the same point as light from more central regions. This would result in loss of focus in peripheral regions. Since the purpose of the confocal pinhole is to remove out-of-focus light, this may also result in loss of signal on peripheral regions of the image. If Plan lenses are not available, which may be the case for low magnification objectives, the confocal software can be used to zoom the image and limit image acquisition to the central area of the objective.

Numerical aperture provides an indication of both the light gathering capacity and resolution of a lens. A brief introduction to resolution with respect to NA is presented at this point to introduce the topic and provide the necessary information to understand the inscriptions on the microscope lenses. A more thorough theoretical discussion of resolution is presented in Chap. 7 which deals with the process of image capture. As NA increases, the number of photons that can be collected by the lens increases, and the resolution the lens is capable of producing is also improved. Key components in determining the NA, as shown in the equation:

$$\mathrm{NA} = n \sin \alpha$$

are refractive index (n) of the medium (air, immersion oil, glycerol or water) between the lens and the coverglass, and the half angle (α) of the cone of light that enters the objective. The significance of the refractive index and examples of refractive index mismatch between the components of the optical path will be discussed in detail in Sects. 3.4.2 and 3.4.3. As discussed in several sections, one of the limiting factors in confocal imaging is the acquisition of an adequate number of photons.

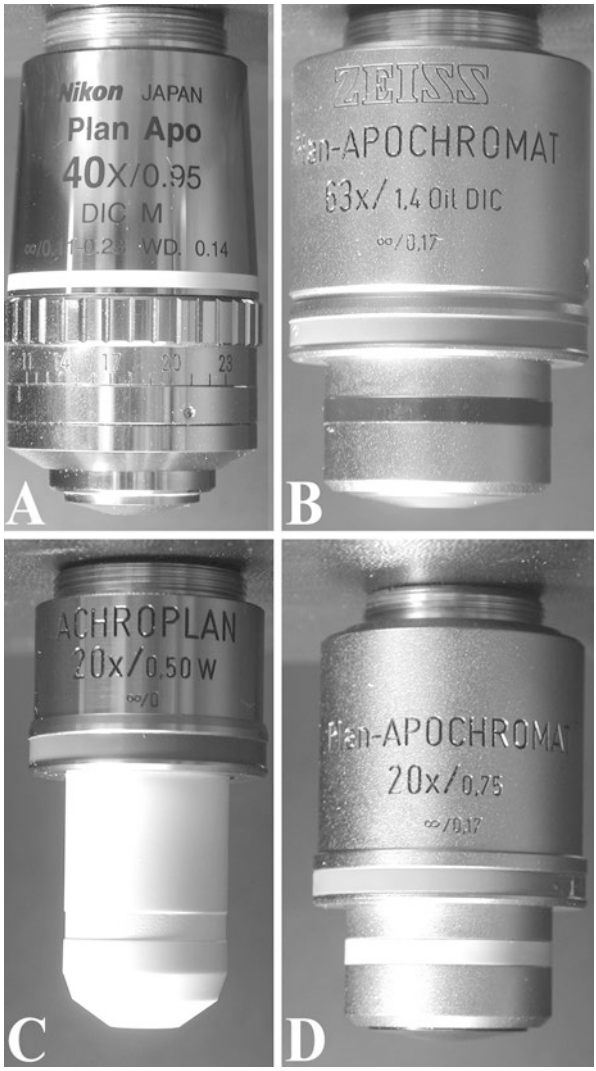

Fig. 3.6 Various types of objective lenses showing inscriptions on the barrel of the objective. (**a**) 40X Plan Apo with correction collar for adjustment to correct for coverglass thickness and refractive index mismatch; (**b**) 63X Plan Apo oil immersion; (**c**) 20X Plan Achromat water immersion; (**d**) 20X Plan Achromat

High NA lenses collect more photons. High NA lenses are also essential for high-resolution confocal imaging as shown in the equation for resolution:

$$d = 0.61\lambda \mathrm{NA}$$

where d is the resolution and λ is the wavelength of the photons. As numerical aperture increases, resolution also improves.

Depth of field (Z) refers to the distance along the vertical or z-axis of the optical path that the specimen, or an object within the specimen, remains in focus. As shown by the equation below, similar to resolution, depth of field is highly dependent on the NA, wavelength of light (λ) used as the imaging source, and the medium between the lens and object (*n*):

$$Z = n\lambda \mathrm{NA}^2$$

As the numerical aperture increases, which is desirable for high-resolution confocal images, the depth through which focused images can be obtained rapidly decreases. This is often a problem with confocal experiments where it is desirable to be able to collect high-resolution 3D z-stacks of images, but the required use of high NA oil immersion objectives limits the depth from which images can be collected.

Depth of focus refers to the thickness of the image plane, or depth of the area around an object in an image, that is in focus. Since this refers to an image plane, the position of the object in the specimen is not changed. If the confocal pinhole is set properly and image collected appropriately, the depth of focus in confocal imaging is not as critical as the depth of field.

Infinity-corrected optics are included on nearly all new optical microscopes (1980s and beyond). In infinity-corrected objectives, light leaving the back of the objective does so in parallel rays which do not come to a focal point to form an image until a tube lens (Telan lens) brings the light to a focal point. The advantage of infinity-corrected optics, especially in fluorescence microscopy, is that multiple components such as barrier filters and beam splitters can be placed in the optical path without affecting the parallel paths the light rays take out of the objective lens. After passing through the components of the optical path, the light is then focused by the tube lens. In non-infinity-corrected optics, light is focused to an image after passing through the back focal plane of the objective. This then requires considerable correction to insure all components of the optical path are matched so light diffraction does not occur as light rays pass through filter cubes, beam splitters, and other components of the optics. If all components are not optically matched, a number of image aberrations, as discussed below, can occur.

Immersion objectives are designed to minimize the refractive index mismatch between the components of the lens and other components within the optical path. For example, the optical components of oil immersion objectives are closely matched with that of the coverglass used to mount specimens. This minimizes the refractive index mismatch as excitation photons pass through the objective and coverglass prior to exciting fluorochromes in the specimen. This is also advantageous as emitted photons must also pass through the same glass components of the coverglass and objective lens. Typically oil immersion objectives have a very high numerical aperture (1.3–1.4) which also results in a high-resolution objective.

Other types of immersion objectives also exist. Water immersion objectives closely match the refractive index of the biological components (proteins, nucleic acids, water) by having a drop of water between the objective and the coverglass

rather than using air or oil as the intermediate medium. While water immersion objectives are excellent at minimizing refractive index mismatch between water in the sample and the surrounding media and, thus, allow deeper imaging into tissues, the numerical aperture of these lenses is not as high as those available for oil immersion optics. Objectives are also available for immersion in glycerol to match the mounting medium used for many biological specimens. In addition, some objectives are classified as multi-immersion objectives, and these can be used for various mounting media or dipping lenses which can be placed directly into the buffer mounting medium of the specimen without the use of a coverglass. Immersion and dipping objectives are typically expensive, and cost increases as the numerical aperture and versatility of the lens increases.

The *working distance* of a lens is the distance between the objective and the coverglass (or specimen if using a dipping lens) when the specimen is in focus. Low magnification objective lenses and water immersion lenses typically have a long working distance, while oil immersion lenses have very short working distances. Care must be taken when focusing all objectives, but one must be diligent in making sure short working distance oil immersion objectives do not run into the coverglass of the specimen during focusing. This can damage the specimen but, more importantly, it can damage the objective. A potential problem that exists with automated microscope systems is the use of samples of varying thicknesses with objectives of different working distances. One should always focus a new sample at low magnification (i.e., 10X) prior to using a short working distance lens. An example of a potential problem with the fully automated Zeiss microscope in our core facility is that a number of investigators utilize the 63X NA 1.4 oil lens to image co-localization in cells cultured on coverglasses. Other investigators may use the same objective to image the surface of sectioned samples that are several microns thick. Since the automated system brings the focal point back to the one previously used, it is essential that those using thick specimens first focus their sample at low magnification. Otherwise, the automatic setting might crash the short working distance objective into the sample.

Wavelength-Corrected Objectives and Chromatic and Spherical Aberrations One of the most important characteristics of an objective used for acquisition of confocal images is the range of wavelengths of light for which it is optimized to collect. Since wavelengths of photons emitted from different fluorochromes vary, the focal point of each after it passes through the objective lens will also differ. It is essential to use objectives corrected for the various fluorochromes being used so that all are focused in the same optical plane. If the fluorochromes are focused in different optical planes, chromatic and spherical aberrations are introduced into the image which can affect data interpretation as discussed in Sects. 3.4.2 and 3.4.3.

On the barrel of the objective lens, inscriptions indicate the level of correction. Achromat lenses are designed to minimize chromatic aberrations in the blue and red wavelengths and spherical aberration in green wavelengths of light. Fluor objectives are also corrected for chromatic aberration in blue and red but are also corrected for

spherical aberration in these ranges. Apochromat objectives are corrected for chromatic aberration for red, green, blue, and possibly UV light and spherical aberration for red and green light. In addition to these basic classifications, there are specialized objectives such as the C-Apochromats for up to six color correction in water immersion lenses which have been introduced for specific uses. These are critical for confocal work involving collection of multiple wavelengths, particularly within the red part of the spectrum. However, even with advanced correction, it is essential that care be taken when interpreting multicolor data as shown in the next several examples.

3.4.2 Effects of Chromatic Aberration

Use of lenses not specifically corrected for collection of multiple wavelengths of light may result in the introduction of chromatic aberration in the image. This can result in image artifacts and improper interpretation of data. Figure 3.7 diagrammatically illustrates the effects of chromatic aberration on the imaging of photons of different wavelengths. In objectives that have longitudinal (axial) chromatic aberration (Fig. 3.7a), photons of shorter emission wavelengths (blue) are focused closer to the objective than those of longer wavelengths (green or red). As shown in Fig. 3.7b, lateral chromatic aberration may result in a change in magnification with shorter wavelengths of light being magnified more than long wavelengths by 1–2%. The correction of chromatic aberration is typically accomplished in the design of the objective by inclusion of multiple lens elements with different optical characteristics. This results in different wavelengths of light being brought into focus in the same plane.

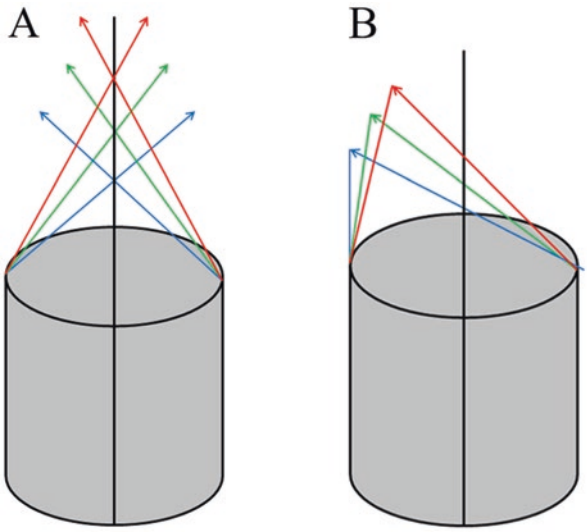

Fig. 3.7 Diagrams of the effects on focal plane and magnification of longitudinal (**a**) and lateral (**b**) chromatic aberrations

Chromatic aberrations may result in two types of defects in the image. First, since out-of-focus photons are removed from the image by a pinhole, the resulting signal will be significantly reduced in the wavelengths that are out of focus. The second artifact may result in a misinterpretation of co-localization data since photons of different wavelengths that are imaged from a single point in the specimen will be out of register in the X-, Y-, and Z-directions and observed as being in different points in the specimen. If working at low magnifications where Z-resolution is relatively poor, this may not be significant. This is why many low magnification objectives are not highly corrected for chromatic aberrations. However, in high-resolution confocal imaging, it is essential that highly corrected objectives be used for collection of images from samples labeled with multiple fluorochromes.

The effects of chromatic aberration on the interpretation of co-localization of structures in a sample have been illustrated by Dunn and Wang (2000) as shown in Fig. 3.8. In this set of experiments, both a mirror and fluorescent beads were imaged with 40X Fluor and 100X Plan Apo objectives at photon emission values of 520 nm, 600 nm, and 680 nm (Fig. 3.8a). With the Plan Fluor objective corrected for red and green emission, these two colors were co-localized, while the emission at 680 nm was displaced by 1.2 μm along the Z-axis. With the Plan Apo 100X objective, which was corrected for all three wavelengths of light, the signals coincided. To demonstrate this effect in a biological sample, the authors simultaneously labeled transferrin (Tf) molecules in cell endosomes with fluorescein, rhodamine, or Cy5. Since there is a very high expression of Tf sites available in these cells, a high probability for double label co-localization exists. In this case, true co-localization of the structures should be observed in the images if no longitudinal chromatic aberration is present. In Fig. 3.8b–d the Plan Apo 100X objective was used to image fluorescein (520 nm emission) and Cy5 (680 nm emission). With this objective, images correctly show a high coincidence in signal localization and intensity indicating that the fluorochromes are co-localized as indicated by the yellow color in Fig. 3.8b and the arrows in Fig. 3.8c and d.

The same sample was then imaged with the 40X Plan Fluor objective corrected for green (fluorescein) and red (rhodamine) emission. Fig. 3.8e again shows the co-localization of these two signals collected with an objective corrected for these fluorochromes. However, when the 40X Plan Fluor objective was used to collect fluorescein and Cy5 signals and the images overlaid, the Tf molecules no longer appeared co-localized. With this objective the image had distinct red and green colors indicating no co-localization (Fig. 3.8f). When a Z-series was collected (Fig. 3.8g) and projected, the signals again appeared co-localized indicating a shift in the Z-positioning of the emitted photons. When the individual fluorescein images collected in Fig. 3.8f were shifted 1.2 μm in the Z-direction, the fluorescein and Cy5 signals correctly appear co-localized (Fig. 3.8h). Fig. 3.8i and j shows that if the same focal plane is collected in the fluorescein and Cy5 channels and shown side-by-side, poor image registration of the Tf labeling results. However, if the fluorescein image is collected at a depth of 1.2 μm greater, there is perfect registration of the signal.

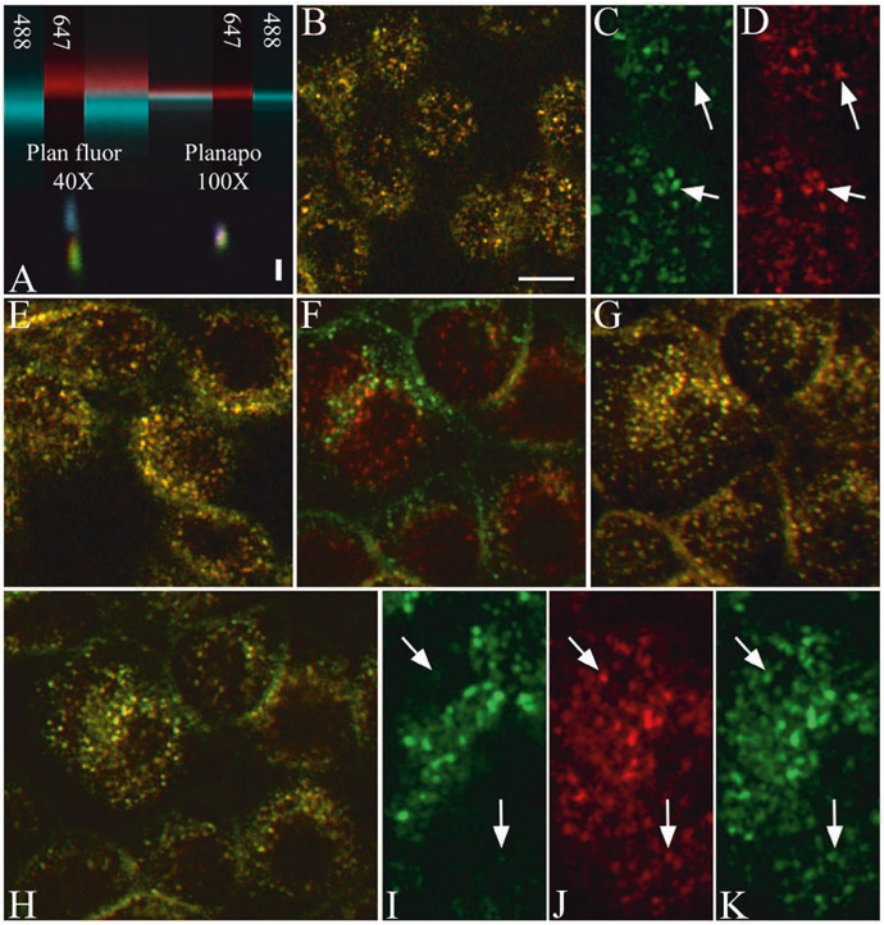

Fig. 3.8 Chromatic aberration in confocal microscopy. (**a**) XZ-sections of glass reflection (top) and microsphere fluorescent (bottom) images collected with a poorly color-corrected Plan Fluor 40x objective (left) and a well-corrected Plan Apochromat 100x objective (right). In the reflection images at the top of this panel, 647 nm light is shown in red, and 488 nm light is shown in blue. In the fluorescence images of fluorescent beads, 520 nm emissions are shown in green, 600 nm emissions are shown in red, and 680 nm emissions are shown in blue. For all images, the focal axis is oriented vertically, with the sample bar indicating a distance of 1 μm. (**b**) An image of a field of cells labeled with both fluorescein-Tf and Cy5-Tf collected with the 100X Plan Apochromat objective. Higher magnification images of the component green and far-red fluorescence are shown in Panels **c** and **d**, respectively. (**e**) An image of a field of cells labeled with fluorescein-Tf and rhodamine-Tf collected with a 40x Plan Fluor objective. (**f**) An image of a field of cells labeled with both fluorescein-Tf and Cy5-Tf collected with the Plan Fluor objective. (**g**) The projection of the vertical series of images from which Panel **f** was obtained. (**h**) The same field shown in **f** but combining green and far-red planes collected at 1.2 μm apart. Higher magnification images of the green and far-red fluorescence from the same focal plane are shown in Panels **i** and **j**, while Panel **k** shows the green fluorescence from a focal plane 1.2 μm lower. Scale bar in **b** represents a 10 μm length for Panels B–H, 5 μm in length for Panels **i–k.** (Used with permission of the authors and Biotechniques, 2008)

In the above set of experiments, a 100X Plan Apo objective corrected for common fluorochromes in the 500 nm through 680 nm emission range was used. With the development and addition of new lasers that have extended the range of fluorochromes that can be used in confocal microscopy, additional care must be taken when selecting fluorochromes for co-localization studies. In a set of experiments similar to those above, we have used a Zeiss Plan Apo 63X objective to image F-actin in cardiac myocytes labeled with 405 nm and 633 nm phalloidin. A similar assumption to the transferrin model above is made here in that both fluorochromes should be co-localized on the F-actin. As above, this Apochromat objective is corrected for fluorochromes emitting in the 500 nm through 700 nm range, it is not well corrected for fluorochromes such as the 405 nm fluorochrome excited with the 405 nm diode laser which emits in the 475 nm range. As a result, the two signals are not co-localized in the image even though they are labeling the same structures (Fig. 3.9). As near-UV lasers become more common on many confocal systems,

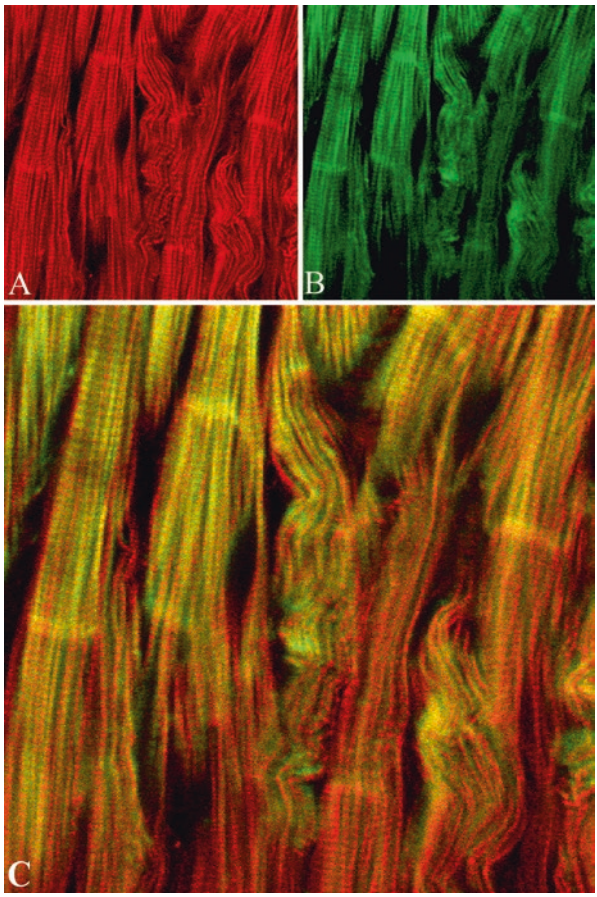

Fig. 3.9 A section of adult mouse heart labeled with 633 phalloidin (**a**) and 405 phalloidin (**b**). Both are labeling f-actin in the cardiac myocytes, but due to chromatic aberrations in the system, the red and green signals do not show 100% overlap

care must be taken in selection of fluorochromes used in co-localization studies to insure they match the lasers and optics of the available confocal microscope.

These experiments clearly show the importance of knowing both the objective lens and fluorochrome characteristics when designing an experiment. When dealing with co-localization data, it is important to be aware of the possibility of aberration and select fluorochromes for which objectives are available to adequately correct for focal shifts due to differing wavelengths.

3.4.3 Refractive Index Mismatch and Spherical Aberrations

As illustrated previously, refractive index mismatch is a primary cause of spherical aberration in microscope systems. This type of aberration results in peripheral rays of light that enter an objective being focused at a different point than the central rays of light that enter (Fig. 3.10). This may result in blurring of the image and significant loss of signal as the confocal pinhole effectively removes the out-of-focus light from the image. Much of the refractive index mismatch that occurs in a confocal system results from differences in the refractive indices of air or immersion oil and common specimen mounting media that are primarily water based, such as the 1:1 PBS:Glycerol mix used in many laboratories.

To address problems with refractive index mismatch, immersion lenses may be used. By utilizing immersion fluids rather than air as the interface between the lens and the specimen, a closer match in the refractive indices in the optical path occurs. This can significantly improve resolution as in the case of high NA oil immersion objectives or depth of imaging in the case of water immersion optics. Similar to

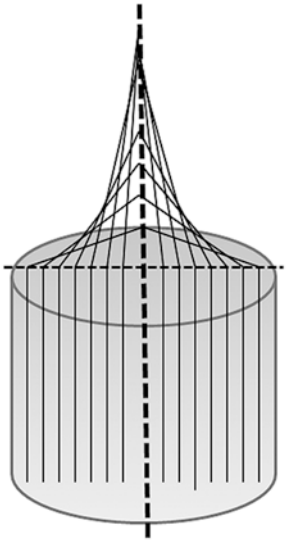

Fig. 3.10 Diagram showing the effects of spherical aberration resulting in peripheral rays of light being focused closer to the objective lens surface than rays of light coming through the central regions of the lens

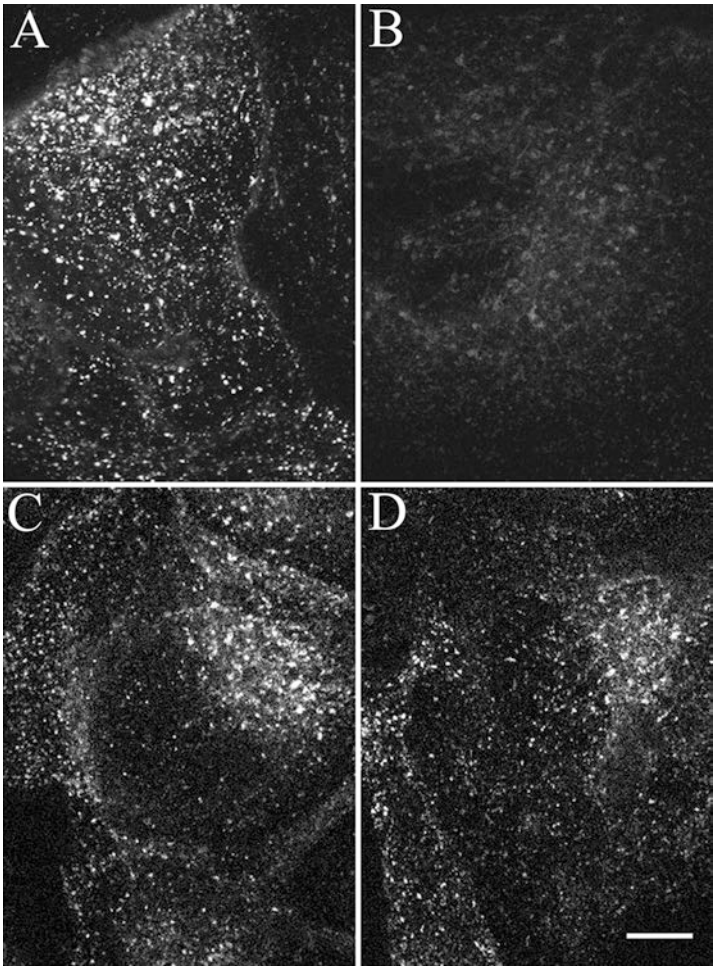

Fig. 3.11 Spherical aberration in confocal microscopy. Images of cells labeled with F-Tf and imaged with either the 100x Plan Apochromat oil immersion objective (**a** and **b**) or the 60X Plan Apochromat water immersion objective (**c** and **d**). Endosomes were imaged at the surface of the coverslip Panels **a** and **c** or at a depth of 35 μm (Panel **b**) or 66 μm (Panel **d**) into the aqueous sample medium. Scale bar is 10 μm in length. (Used with permission of the authors and Biotechniques, 2008)

their experiments demonstrating the effects of chromatic aberrations, Dunn and Wang (2000) have also used fluorescein-Tf-labeled endosomes to demonstrate the effects of refractive index mismatch by imaging the same sample with a 100X Plan Apochromat oil immersion objective and a 60X Plan Apochromat water immersion objective (Fig. 3.11). When imaging near the surface with the 100X Plan Apochromat oil immersion objective, a strong signal can be obtained. However, due to refractive index mismatch between the immersion oil and the water-based mounting medium

of the sample, signal is rapidly lost due to spherical aberration as imaging depth is increased (Fig. 3.11 a–b). At a depth of only 35 μm, essentially no signal was available for imaging. When using the 60X Plan Apochromat water immersion lens, which minimizes refractive index mismatch between the immersion and mounting media, excellent images were obtained 66 μm deep in the specimen (Fig. 3.11 c–d).

In addition to spherical aberrations associated with refractive index mismatch between the immersion and mounting media, depth of imaging, even with water immersion optics, can be dramatically affected by the specimen itself. One of the common questions asked by investigators beginning confocal imaging is how deep can I image into my specimen? As seen above, knowing the specifications of the objective being used is important in answering this question. Equally important is a basic knowledge of the characteristics of the specimen being imaged. Figures 3.12 and 3.13 illustrate the effects of specimen (protein?) density on the depth of imaging. In Fig. 3.12 Cy3-phalloidin was used to label the somites of a chicken embryo, which was then imaged with 20X NA 0.75 air and 20X NA 0.5 water immersion objectives. With the 20x air objective, signal was significantly decreased at a depth of 100 μm in the specimen. However, with the water immersion objective, a strong

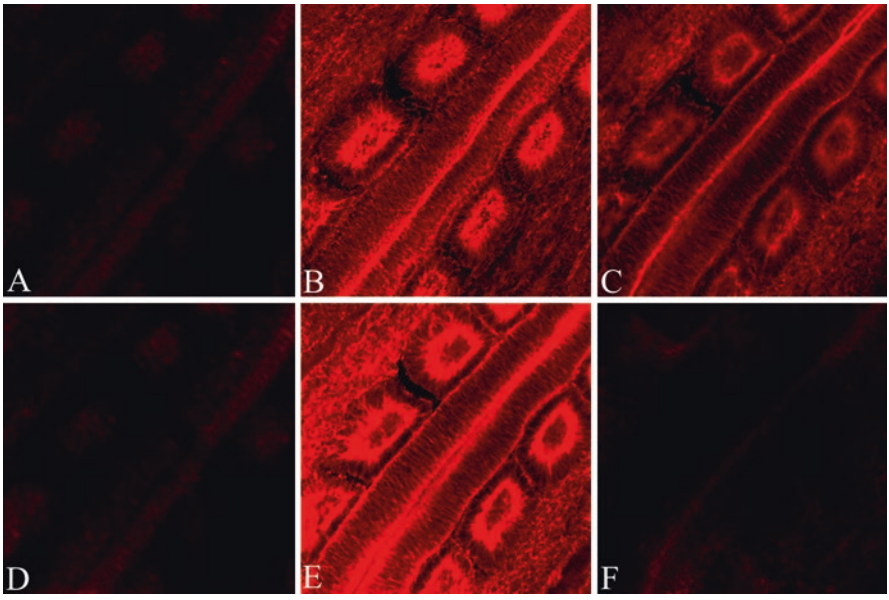

Fig. 3.12 Effects of refractive index mismatch on depth of imaging. A 200 mm thick section of mouse embryo was labeled with Alexa 543-phalloidin (red channel) and somites imaged with a 20x NA 0.5 water immersion lens (**a**–**c**) and a 20X NA 0.75 dry lens (**d**–**f**). A Z-series was collected with image acquisition optimized for collection at 50 μm deep in the sample. Images **a** and **d** were collected at the surface of the sample, images **b** and **d** 50 μm deep, and **c** and **f** 100 μm deep With the 20X dry objective, all signal was lost at 100 μm into the section, while a strong signal was still present at this depth with the 20X water immersion objective. Signal was not lost with this objective until a depth of 150 μm was imaged

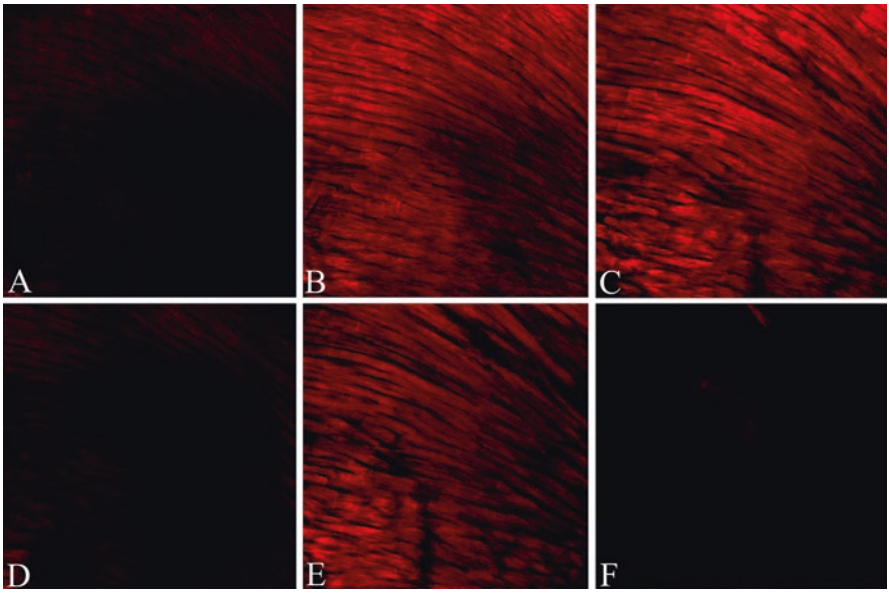

Fig. 3.13 Effects of refractive index mismatch and tissue density on depth of imaging. A 100 μm thick section of mouse heart was labeled with Alexa 543-phalloidin (red channel) and myocytes imaged with a 20x NA 0.5 water immersion lens (**a**–**c**) and a 20X NA 0.75 dry lens (**d**–**f**). A Z-series was collected with image acquisition optimized for collection at 15 μm deep in the sample. Images **a** and **d** were collected at the surface of the sample, images **b** and **d** 14 μm deep, and **c** and **f** 28 μm, deep. With the 20X dry objective, all signal was lost at 28 μm into the section, while a signal was still present at this depth with the 20X water immersion objective. Signal was not lost with this objective until a depth of 50 μm was imaged. Compare this to the results of imaging depth with embryonic tissue which could be imaged much deeper into the specimen

signal was still available at this depth, and signal did not decrease until a depth of 150 μm was tested.

Using the same 20X optics and Cy2-phalloidin label, we also imaged adult mouse heart, which is a much denser sample than the embryonic tissue imaged above. With this sample signal was lost at a depth of less than 25 μm with the 20X dry lens but was still strong with the water immersion lens at this depth (Fig. 3.13). Imaging depth of dense adult cardiac tissue was approximately 25% of that obtainable with embryonic tissue using the same preparation protocols and optics illustrating the importance of knowing specimen characteristics in addition to optical specifications when determining imaging parameters.

In response to the need to image as deep as possible into tissue, a number of techniques have recently been developed to clear tissues, and these will be discussed in detail in Chap. 4. To enhance one of these techniques, X-CLARITY, Leica has also developed an objective (Fig. 3.14) to match the refractive index of the mounting medium used in the process, which also closely matches the refractive index of biological tissues. An example of the increased imaging depth possible with this technique is shown in Fig. 3.15 where it was possible to image mCherry-

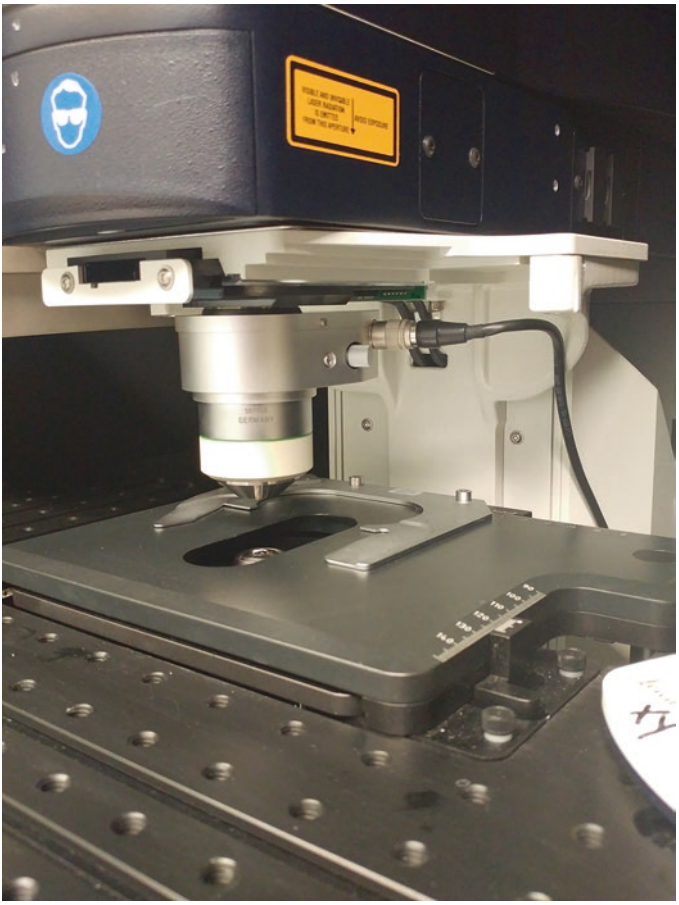

Fig. 3.14 Leica CLARITY objective mounted on an SP8 upright confocal system

labeled cells through 960 μm of tissue. Without clearing it is difficult to image through more than 50 μm of adult brain.

An additional factor that affects spherical aberration is the thickness of the coverglass since this affects the length of the optical path through the glass. Most modern microscope lenses are corrected for a number 1.5 coverglass, and this is the thickness of coverglass that should be employed unless a specific lens indicates otherwise. However, even within a batch of #1.5 coverglasses, there can be small but important differences in thickness. While it may not be practical to measure the actual thickness of every coverglass used, one must be aware that minimal variations in the thickness of a coverglass can affect image quality and interpretation. Manufacturers have addressed this problem, as well as the above factors affecting spherical aberrations, by providing objectives with correction collars. Correction collars can be adjusted to accommodate small variations in coverglass thickness and

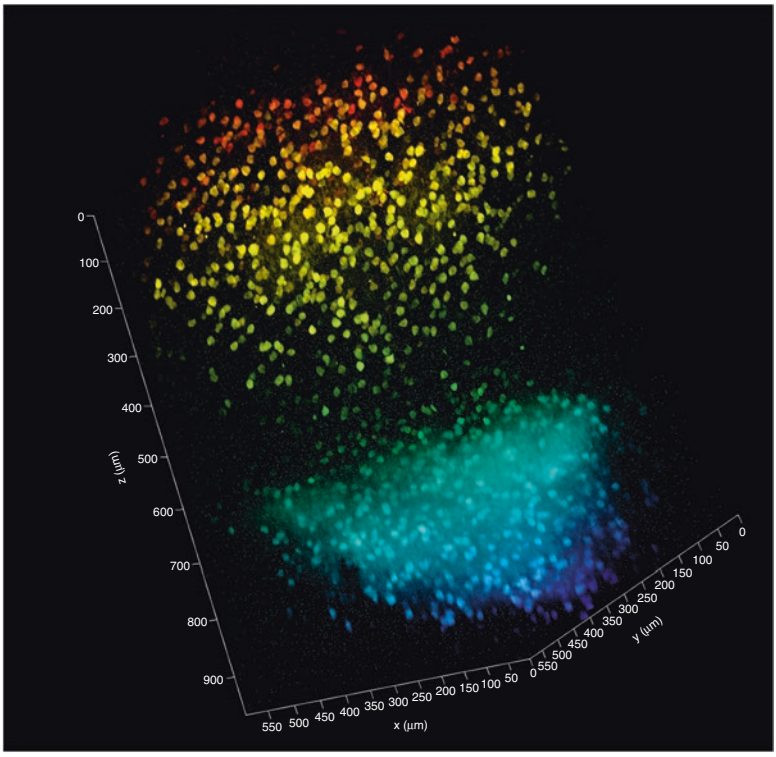

Fig. 3.15 Cleared slice of adult mouse brain stained with mCherry. It was possible to obtain signal 960 µm into the slice although spherical aberration started affecting resolution at approximately 500 µm as shown by the reduced sharpness (resolution) at that level. Signal also began to deteriorate as shown by the increased background level at approximately 600 µm deep

minimize image aberrations. While fairly expensive, these objectives are ideal for imaging deep into a specimen with minimal spherical and chromatic aberration as shown by another set of experiments performed by Dunn and Wang (2000). Using a 60X water immersion objective with a correction collar, they first collected a set of cross-sectional images from a glass surface at 488 nm and 647 nm at both the surface and at a depth of 63 µm in an aqueous medium (Fig. 3.16a). The signal from these two wavelengths differed by a depth of 0.6 µm in both cases indicating the shift in Z-direction was not due to imaging depth.

They then collected images from a triple labeled bead with emissions at 520 nm (green), 600 nm (red), and 680 nm (blue). With the correction collar adjusted for a measured coverglass thickness of 174 µm, the green and red signals coincided, while the blue signal was offset, as expected from the measurements made from glass. When the correction collar was purposefully misadjusted for a 150 µm coverglass to introduce spherical aberration, the red and green signals no longer coincided, and image intensity was significantly reduced. This type of error is often

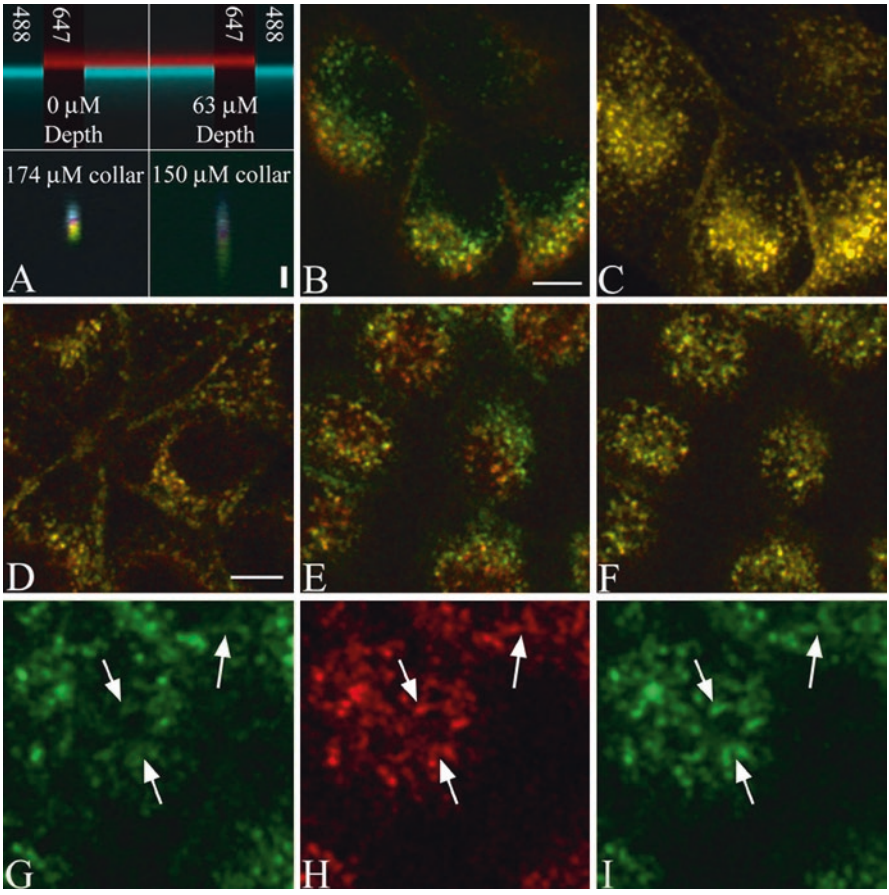

Fig. 3.16 Chromatic aberration in the 60X Plan Apochromat water immersion objective. (**a**) XZ-sections of glass reflection (top) and microsphere fluorescence (bottom) images. Reflection images are shown for depths of either 0 or 63 µm into an aqueous medium, with 657 nm light shown in red and 488 nm light shown in blue. Fluorescence images of fluorescent beads are shown for an objective with correct (left) and incorrect (right) coverslip-thickness collar setting. With 520 nm emissions shown in green, 600 nm emissions shown in red and 680 nm emissions shown in blue. For all images, the focal axis is oriented vertically, with the scale bar indicating a distance of 1 µm. (**b**) An image of a field of cells labeled with F-Tf and Cy5-Tf collected at a depth of 63 µm into an aqueous medium. (**c**) The projection of the vertical series of images from which Panel B was obtained. (**d**) An image of a field of cells labeled with fluorescein-TF and rhodamine-Tf collected at the coverslip surface. (**e**) An image of a field of cells labeled with both fluorescein-Tf and Cy5-Tf collected at the coverslip surface. (**f**) The same field shown in Panel E but combining green and far-red planes collected 0.6 µm apart. Higher magnification images of the green and far-red fluorescence from the same focal plane are shown in Panel **g** and Panel **h**, while Panel **i** shows the green fluorescence from a focal plane 0.6 µm lower. Scale bar in Panel **b** represents 10 µm length in Panels **b** and **c**. The scale bar in Panel **d** represents 10 µm length in Panels **d**–**f** and 5 µm in Panels **g**–**i** (Used with permission of the authors and Biotechniques, 2008)

encountered since the thickness of coverglasses from a single batch may vary by up to 40 μm around the thickness value at which they are sold.

To further demonstrate how these optical effects might lead to misinterpretation of co-localization data, Dunn and Wang (2000) again collected a series of images from Tf-labeled endosomes. In this set of experiments, they utilized the 60X water immersion lens and imaged through aqueous media at a depth of 63 μm. In Fig. 3.16b, a chromatic shift was present when imaging with fluorescein- and Cy5-labeled Tf. However, by projecting a Z-series of the images (Fig. 3.16c), the chromatic shift is no longer apparent, and the Tf molecules properly appear co-localized.

Consistent with data presented in Fig. 3.16a, when fluorescein- and rhodamine-labeled Tf molecules are imaged at the surface of the sample, they appear co-localized (Fig. 3.16d). However, even though imaging is at the surface of the sample, when fluorescein- and Cy5-labeled Tf molecules are imaged, there again is a chromatic shift indicating labeling of discrete populations of endosomes (Fig. 3.16e). If the fluorescein image is again collected 0.6 μm deeper, the co-localization is again apparent (Fig. 3.16f). Figures 3.16g–i show separate channels for fluorescein (Fig. 3.16g), Cy5 (Fig. 3.16h), and fluorescein collected 0.6 μm deeper (Fig. 3.16i) to further illustrate the mis-registration of images due to spherical aberration.

The examples above demonstrate the critical importance of carefully selecting and knowing the specifications of the objective lenses used in confocal and fluorescence imaging. Co-localization studies are common in confocal microscope experiments, and misinterpretation of co-localization data can easily occur if lenses are not corrected for the wavelengths of fluorochromes being used. Another common application of confocal systems is three-dimensional reconstruction of data sets. To optimize these experiments, minimizing spherical aberration in the optical path is essential in maximizing the usefulness of the confocal system.

3.5 Filters

In fluorescence microscopy filters are usually necessary for insuring that only light emitted by a fluorochrome in the sample is passed on to the detector and for blocking any stray light in the system. In addition, filters are needed to separate the various wavelengths of light emitted from different fluorochromes when using multiple fluorochromes emitting at different wavelengths. Finally, in situations where non-monochromatic light is used for excitation, filters are necessary for restricting the excitation wavelengths to only those necessary for excitation of the fluorochrome and restriction of the wavelengths that might be mistaken for emitted photons. Even when the emitted wavelengths have a narrow range, such as with lasers or LED arrays, it is usually desirable to include emission filters to restrict stray light entering the system. Also, since lasers generally have multiple narrow emitted wavelengths (Fig. 3.4), filtering helps insure that only the laser line of interest is part of the light path.

Basic filters can be classified roughly as short-pass filters (also known as low-pass filters), long-pass filters (also called high-pass filters), and band-pass filters. A long-pass filter (Fig. 3.17a) blocks all light below a certain wavelength and transmits wavelengths longer than that cutoff. Conversely, short-pass filters (Fig. 3.17b) transmit wavelengths shorter than the cutoff and block longer wavelengths. Band-pass filters (Fig. 3.17c) pass light within a certain range of wavelengths and block all wavelengths above and below that range.

For a long-pass filter, the filter is named by the wavelength at which 50% of its peak transmittance is passed. Figure 3.17a shows the transmission curve for a 459 nm long-pass filter. The filter transmits only 1% of 450 nm light that reaches the filter. However, 92% of 500 nm light passes through the filter. This is the maximum transmittance for this filter. The half maximum value is 46%, and this value is attained with light having a 459 nm wavelength. The filter would thus be designated a 459 nm long-pass filter. Similarly, short-pass filters are named for the wavelength at which 50% of their peak transmittance is blocked.

Band-pass filters transmit a range of wavelengths. The range can be very narrow, as is the case for the filter depicted in Fig. 3.17c, or the spectrum can be broad. Band-pass filters are designated by their central wavelength and the range of wavelengths they transmit. The lower and upper boundaries of the range are determined as the wavelength at which the half maximal values are achieved. This is often referred to as the full width half maximal (FWHM) value (double arrow in Fig. 3.17c). The central wavelength is the arithmetic mean of the upper and lower boundaries. For the filter depicted in Fig. 3.17c, the peak transmittance is 87%. Half of this value, 43.5% is attained at 528 nm and 554 nm. The arithmetic mean of 528 and 554 is 541 and the range from 528 nm to 554 nm is 26 nm. The filter would thus be designated as a 541/26 nm band-pass filter.

Fluorescence microscopy also requires that the excitation beam and emission beam are ultimately separated from each other. The most common method is to employ a specialized type of filter called a dichromatic beam splitter (also known as a dichroic mirror). Most filters are designed to have a zero angle of incidence. This is the angle between the optical axis of the incident light and the angle normal to the filter surface. The dichromatic beam splitter is designed for high incidence angles, usually 45 degrees. The beam splitter reflects light of short wavelengths and passes light of longer wavelengths, thus separating higher and lower wavelengths.

Figure 3.1 shows the filter arrangement in a standard epifluorescence microscope using an arc lamp source. An excitation filter (usually a band-pass or, sometimes, a short-pass filter) limits the wavelengths of light that illuminates the specimen. This helps make sure that only the desired fluorophore is excited. The dichromatic beam splitter reflects this light to the back focal plane of the objective lens which focuses the excitation beam onto the specimen. In a well-designed microscope, very little of this excitation light is reflected back. In this way, only the light emitted from excited fluorophores is collected and focused by the objective lens. The emitted photons travel back to the dichromatic beam splitter. Since these have a longer wavelength than the excitation light, they are transmitted through the dichromatic beam splitter, while any stray excitation light, because of its shorter wavelength, is reflected by the

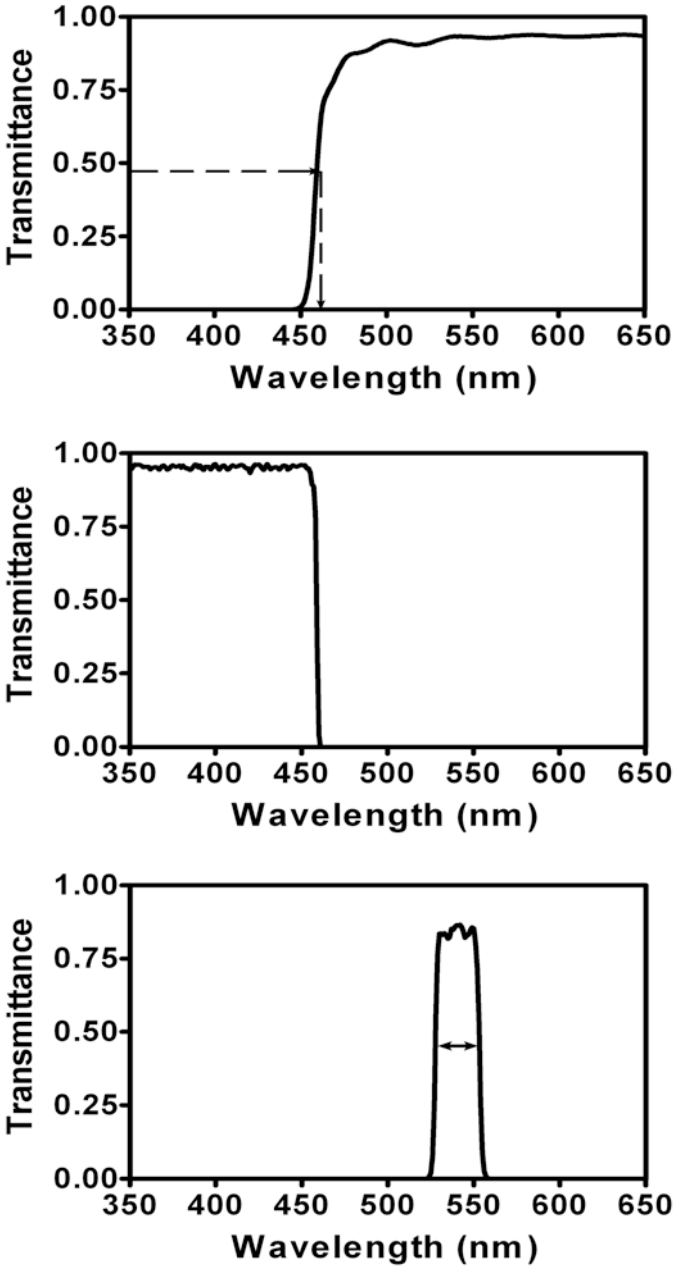

Fig. 3.17 Spectra for typical long-pass (**a**), short-pass (**b**), and band-pass (**c**) filters

dichroic back toward the light source. A filter on the other side of the dichromatic beam splitter helps to further limit the wavelengths that reach the detector to only those emitted by the fluorochrome. This emission filter (also called a barrier filter) is usually a long-pass or band-pass filter.

3.6 Types of Filters

3.6.1 Glass Filters

A variety of devices are available that discriminate and separate different wavelengths. The most common are colored glass filters. These are inexpensive, have long useful lives, and they are relatively insensitive to incidence angle. However, there are limitations to glass filters. Chief among them are low transmittance and high autofluorescence at longer wavelengths. Thin film interference coatings are an alternate method of making filters. These have high transmittance and can be designed to provide a wide variety of filtering parameters. The drawbacks of thin film coatings are that (1) their blocking performance holds for only specific wavelengths so other blockers must often be added, (2) they are very sensitive to angle of incidence, and (3) coatings that work well for visible light are usually not ideal for UV and so UV performance is compromised.

Filters that attenuate the intensity of the signal (called neutral density filters) are also useful for controlling the intensity of light on the specimen. This is particularly important for lasers, since they are high-intensity sources. While the high intensity of lasers can be an advantage in exciting fluorochromes and generating high signal levels, in many cases the intensity is so high that it is desirable to attenuate or decrease the intensity of light entering the optical path. Control of the intensity of light on the excitation side of the optical path is necessary to minimize photobleaching of the sample and to prevent cell death when imaging living samples. In early generation instruments, this was accomplished by placing a neutral density filter in front of the laser to decrease the amount of light entering the scan head. For instance, in the BioRad MRC 1024 line of instruments, neutral density filters that allowed 0.1%, 0.3%, 3%, 10%, 30%, or 100% (no filter) of the laser light through were options when imaging a sample. When samples were either very bright or susceptible to photobleaching or death, filters that allowed small percentages of laser light through to the sample could be selected. When samples generated a relatively poor signal, neutral density filters that allowed more excitation photons into the optical path could be used to improve the signal generated from the sample. However, this method of controlling the amount of excitation light contacting the specimen was limited in the selection of intensity level and also resulted in excitation of the entire sample area; no imaging could be done on smaller regions of interest (ROI).

3.6.2 Acousto-optical Tunable Filters (AOTF)

Most newer laser confocal systems utilize acousto-optical tunable filters (AOTF) to provide precise control of the laser intensity and the region of interest (ROI) in the sample that is excited. AOTF assemblies consist of a quartz filter subjected to various levels of ultrasound. By adjusting the intensity of the ultrasonic wave, the intensity of the laser light passing through the quartz can be adjusted between 0% and 100% in 0.1% increments. This provides very precise control over the intensity of light entering the optical path. In addition, selection of single or multiple excitation wavelengths of light for excitation is much easier with an AOTF than with a filter wheel containing multiple excitation filters. This is an important advantage when imaging multiple fluorochromes either simultaneously or sequentially.

An additional advantage of AOTF systems is that specific ROIs can be selected for excitation while the remaining areas of the sample are not exposed to excitation photons (Fig. 3.18). This is often important in samples that are sensitive to intense beams, such as living cells, since regions of the specimen outside the area of

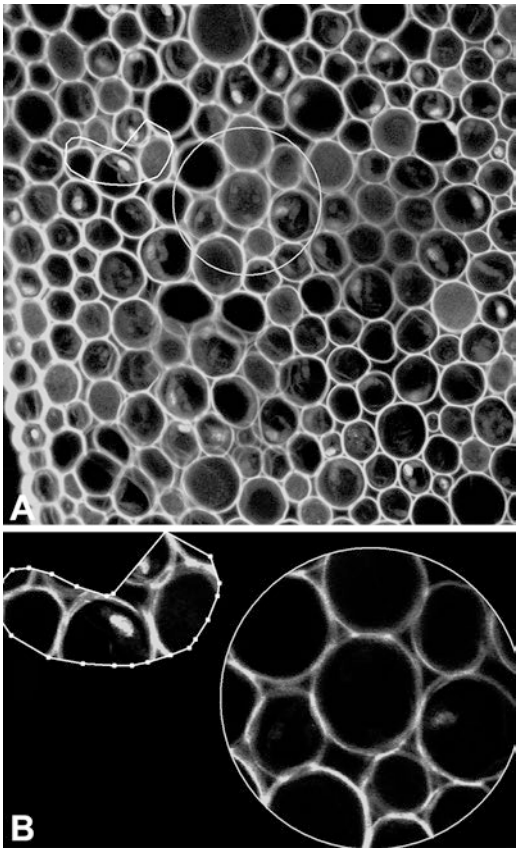

Fig. 3.18 Illustration of selection of ROI areas for scanning to increase the speed of scanning in select regions and to preserve the specimen in areas outside of the ROI. In **a** the entire specimen (Convallaria root tip) has been scanned and then a standard circle ROI and a hand-drawn ROI selected and scanned as shown in **b**

excitation are not illuminated and thus escape any damage. Region of interest imaging is also very useful for applications that involve rapid processes or restricted illumination of only small areas of the sample such as Förster resonance energy transfer (FRET) or fluorescence recovery after photobleaching (FRAP).

3.6.3 Acousto-optical Beam Splitters (AOBS)

There are several potential problems with the dichroic filters that are commonly used to sort the excitation and emission photons in wide-field fluorescence and confocal microscopes. In many confocal studies, multiple fluorochromes are used, and this requires the use of a series of filters in order to adequately separate the excitation and emission wavelengths of the multiple fluorochromes. Typically, the number of filters available in a system is limited, and the ones available may not provide the optimal transmission of photons for the range of fluorochrome wavelengths being generated. Even if multiple dichroic filters are available on a system, it is necessary to mechanically shift between these beam splitters as different fluorochrome excitation and emission wavelengths are generated. Although the filter changes are software driven and relatively fast, they do slow acquisition times when imaging multiple channels. Moreover, the mechanical shifting of filters can introduce vibrations. Finally, glass filters are not absolutely efficient, and so not all incident photons are passed through the filter. This decreases the signal and may adversely affect the signal to noise ratio in the final image.

In 2002, Leica introduced the AOBS as an alternative to dichroic mirrors in their confocal systems (Borlinghaus et al. 2006). Similar to dichroics, the AOBS transmits short excitation wavelengths of light to the specimen and also directs the transmission of longer wavelength photons emitted from the specimen to the detector. However, the AOBS utilizes an electronically tunable acoustic crystal in place of the dichroic mirror and is a fixed device. The ability to electronically tune the AOBS eliminates the need for dichroic mirrors to be mechanically inserted or removed from the optical path. This allows for faster switching between laser excitation wavelengths (lines), the use of up to eight illumination lines simultaneously, and the selection of narrow bands of light (0.6–2.0 nm) for excitation of fluorochromes. All this is done without having to physically move filters.

3.7 Determining an Optimum Filter Combination

Choosing the correct filter set for a given fluorophore is simply a matter of matching the characteristics of the fluorochrome with those of the filters. In Chap. 2, Fig. 2.3 depicts the excitation and emission curves for TRITC. This fluorochrome has a peak excitation at 555 nm and peak emission at 580 nm. The range of excitation

wavelengths at FWHM is 533 nm through 571 nm. To optimize fluorescence the microscopist would like an excitation beam that is within this range and as close to the excitation maximum as possible. However, overlap with the range of emission wavelengths should be avoided. For TRITC, the emission range at FWHM is 563–610 nm. Thus, there is an overlap of the excitation and emission FWHM values between 563 and 571 nm.

A 540/25 nm band-pass filter would limit the excitation light to below the TRITC emission range. The 543 wavelength of a helium-neon laser could also be used for excitation of TRITC. This wavelength is well out of the emission range of TRITC but would promote sufficient absorption. A 565 nm dichromatic beam splitter would reflect the excitation light and pass most of the light emitted from TRITC. Finally, a 575 nm long-pass filter would insure that most of the signal hitting the detector was specifically from the excited TRITC. This of course is not the only filter combination that could be used with TRITC. For instance, a 610/75 nm band-pass filter would also work as a TRITC emission filter as would an optimally tuned AOBS.

For detecting fluorophores of a single wavelength (single color detection), the choice of the filters to use is relatively simple since you do not need to worry about specific excitation of or emission from competing fluorophores. This is not the case when you want to detect two or more fluorophores in a single sample. The presence of multiple fluorophores increases the probability of spectral overlaps. This is a problem because in fluorescence microscopy the detectors most often used do not discriminate between wavelengths (i.e., they do not recognize color); they only record the presence or absence of photons (the standard detectors used in confocal microscopy are described further in Chap. 7). The color specificity assigned to photons is arbitrary but generally based on assumptions about the wavelengths that are transmitted to the detector by the filters that are placed in the light path. If the microscopist has selected these filters incorrectly, spurious interpretations can occur.

Two principal types of artifacts can occur with imperfect filtering when two or more colors of fluorescence are analyzed. The first artifact results when the emission from the first fluorochrome has the proper wavelength to excite the second fluorochrome. This situation is depicted in Fig. 3.19. The emission peak of fluorochrome I falls within the excitation wavelengths of fluorochrome II. Without attention to proper filtration, this scenario could result in the fluorescence coming from both fluorochromes I and II being incorrectly interpreted as coming only from fluorochrome I based on the excitation wavelength employed. However, with a suitable emission band-pass filter, the emission from fluorochrome I can be discriminated from that arising from fluorochrome II as long as there is no substantial overlap of the two emission spectra. Figure 3.20 depicts two hypothetical emission peaks and indicates a band-pass filter which would allow detection of emission from only fluorochrome I. An alternative would be to choose different fluorophores where the emission spectrum of one does not overlap the excitation spectrum of the other. This is the safer alternative.

The second problem in assuring specificity of detection arises when two emission spectra have substantial overlap as shown in Fig. 3.21. If both signals are

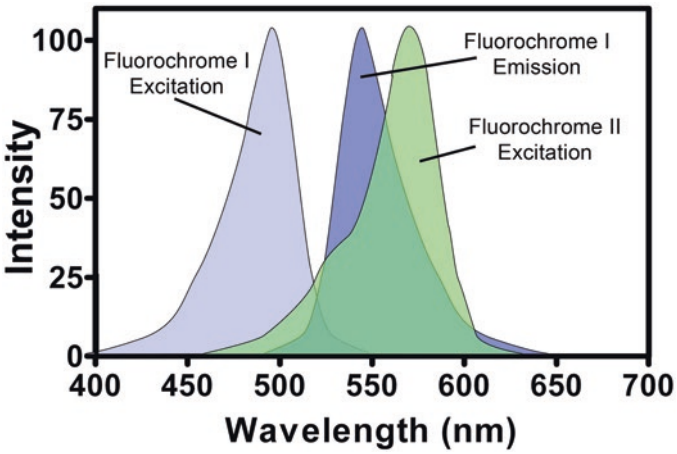

Fig. 3.19 Spectral overlap of emission from one fluorophore with excitation of a second fluorophore

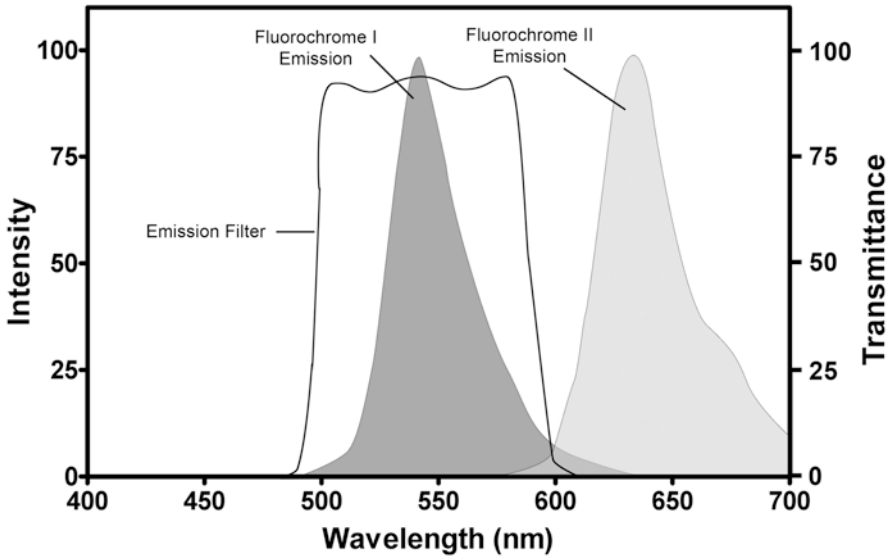

Fig. 3.20 Use of band-pass filter to separate emission of one fluorophore from emission of a second fluorophore when the two fluorochromes have similar excitation spectra

strong, as depicted in Fig. 3.21a, it would not appear that the fluorochrome 1 emission (stars) makes up a substantial component of the emission assigned to fluorochrome II (circles) using a band-pass filter designed for fluorochrome II (in this case a 600/50 band-pass filter). However, if the signal from fluorochrome II is low compared to fluorochrome I, the emission assigned to fluorochrome II could be substantially overestimated (Fig. 3.21b). Moreover, even if fluorochrome II was not present,

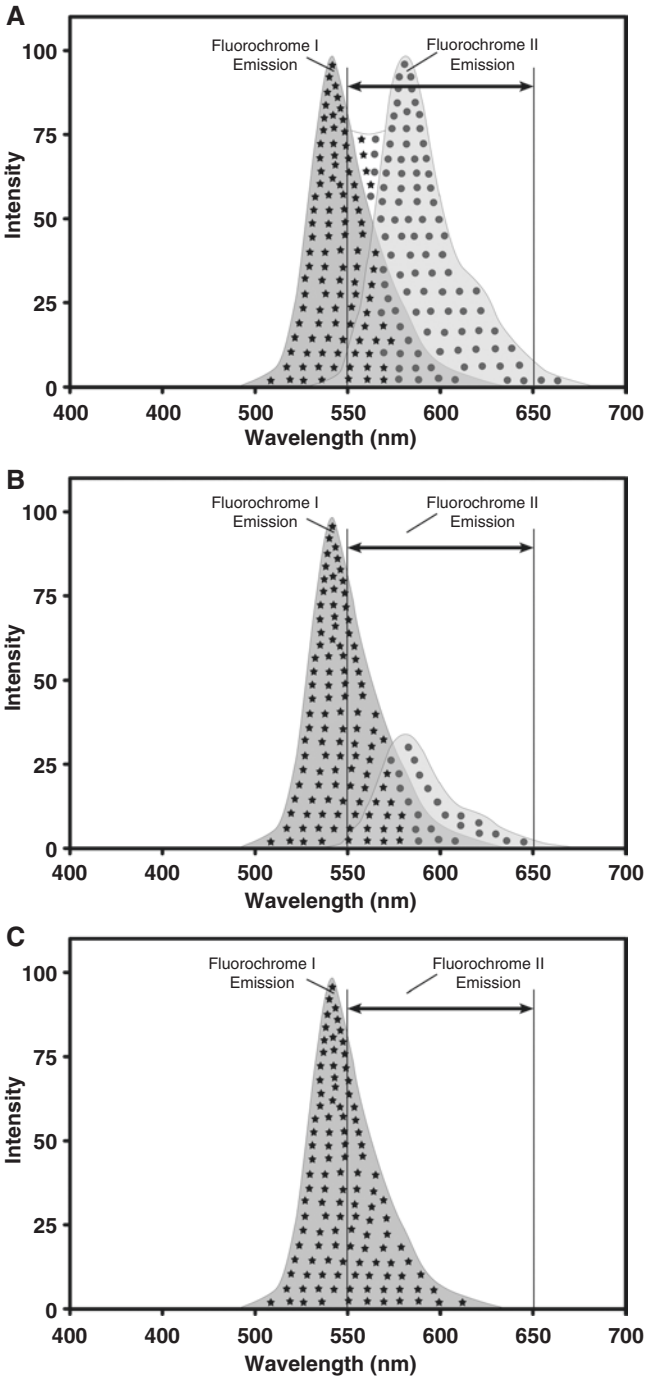

Fig. 3.21 Simultaneous two-color fluorochrome detection and the effect of bleed through of signal assigned to the higher wavelength fluorochrome. (**a**) When the signal from fluorochrome II (circles) is strong, the bleed through of fluorochrome I (stars) has a limited but still significant effect on the signal detected using a 600/50 band-pass filter. (**b**) When the signal strength of fluorochrome II is weak, the bleed through of fluorochrome I becomes the dominant signal. (**c**) When fluorochrome II is not present, bleed through produces a signal that could be spuriously interpreted as the presence of fluorochrome II

a signal would be detected and spuriously assigned to fluorochrome II (Fig. 3.21c). Thus this overlap of emissions (termed bleed through) must be carefully guarded against and proper controls initiated to test for possible overlap. Eliminating bleed through is always important but, as discussed in Chap. 11, it is critical when undertaking co-localization studies.

Of course, to avoid bleed through, one could use narrower band-pass emission filters to collect only photons from the non-overlapping regions, but, as in the example shown in Fig. 3.22, this may substantially reduce the number of photons collected. In fact, the signal could be reduced enough that it is not distinguishable from noise leading to spurious conclusions about the presence or amount of fluorophore present. A better approach is to sequentially excite one fluorochrome and then the other instead of attempting to collect the two signals simultaneously. Sequential collection reduces the necessity to discriminate between two simultaneously excited fluorochromes because it can optimize collection conditions for each fluorochrome separately. Advancements in automation of functions like filter switching and the AOBS make sequential imaging of two or more fluorochromes much faster and easier. Most modern confocal microscopes are ideal instruments for such a sequential approach.

There are also mathematical techniques that attempt to determine the contribution of two or more overlapping fluorophores to a complex spectrum. These techniques, often referred to as spectral analysis or spectral unmixing, are discussed in Chap. 9 and are an advancement found in many laser scanning confocal microscopes produced after 2005. They allow for specific detection of fluorochromes with overlapping spectra. However, by far, the best and easiest approach to separating

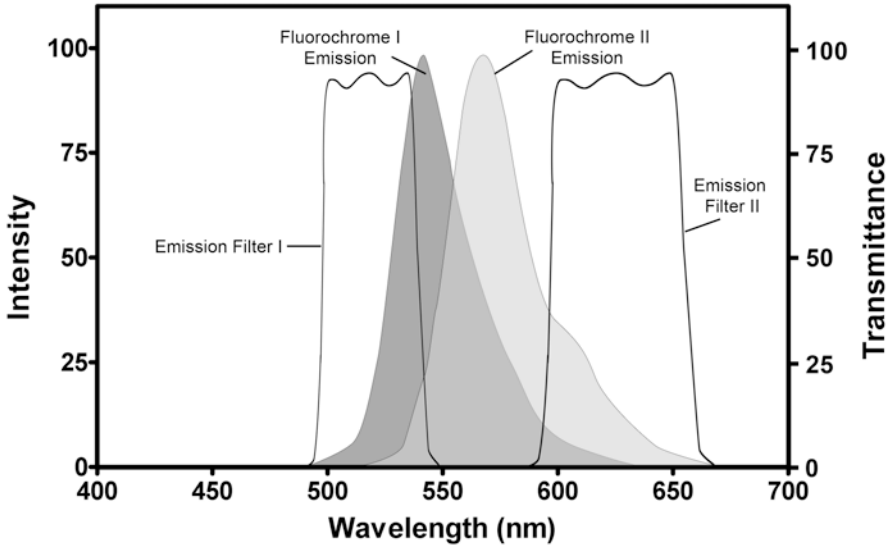

Fig. 3.22 Band-pass filters for separating non-overlapping regions of two fluorophores with overlapping spectra

fluorescent signals is to use fluorochromes with widely separated emission spectra whenever possible.

In all cases, it is necessary to confirm that selected filter combinations are working as expected. This can be done by exciting one fluorochrome at a time while monitoring the emission being transmitted through all the other filter combinations. There should be no signal above background through any of the filter sets other than the one for the fluorochrome of interest.

3.8 Optimizing the Fluorescent Signal

Because of a number of factors, the amount of light reaching the detector in a fluorescence microscope is relatively low. Even with very sensitive detectors, one still must insure that the signal strength is sufficiently high compared to background noise. Otherwise, you cannot be confident regarding the accuracy of what is detected. Throughout the remaining chapters of this book, we will discuss methods to increase the number of photons detected. This aspect of confocal microscopy cannot be overemphasized. "Photons are your friends, don't abuse them!" should become your mantra. In order to maximize signal, it is imperative to carefully review the excitation and emission spectra of the selected fluorophore(s) and choose filters based on these spectra. It is cheaper in the long run to buy additional filters, if needed, than to misinterpret critical data because of sloppy microscopy. Once the correct filters are in place, additional key elements for maximizing signal strength include (1) properly aligning all elements of the excitation and emission pathways; (2) removal of dirt and other obstacles that would impede the flow of photons to the detector; (3) matching, as close as possible, the refractive indices of all parts of the imaging path, including the specimen so that photons are not lost due to refractive index mismatch; (4) minimizing loss of energy to competing processes (e.g., photobleaching) which decrease the fluorescence signal; and (5) using a high numerical aperture lens to collect as much of the emitted light as possible.

Literature Cited

Borlinghaus R, Gugel H, Albertano P, Seyfried V (2006) Closing the spectral gap - the transition from fixed parameter fluorescence to tunable devices in confocal microscopy. Proc SPIE 6090:60900T60901-60906

Diaspro A, Federici F, Robello M (2002) Influence of refractive-index mismatch in high-resolution three-dimensional confocal microscopy. Appl Opt 41(4):685–690

Dunn, KW. And Wang, E. 2000. Optical aberrations and objective choice in multicolor confocal microscopy. BioTechniques 28(3): 542–550

Samoc A, Miniewicz A, Samoc M, Grote JG (2007) Refractive-index anisotropy and optical dispersion in films of deoxyribonucleic acid. J Appl Poly Sci 105:236–245

Voros J (2004) The density and refractive index of adsorbing protein layers. Biophys J 87:553–561